



Design of folic acid decorated virus-mimicking nanoparticles for enhanced oral insulin delivery

Hongbo Cheng, Shuang Guo, Zhixiang Cui, Xin Zhang, Yingnan Huo, Jian Guan, Shirui Mao^{*}

School of Pharmacy, Shenyang Pharmaceutical University, Shenyang 110016, China

ARTICLE INFO

Keywords:

Chitosan
Folate
Insulin
Nanoparticles
Mucus penetrating
Targeting

ABSTRACT

Mucus penetration and intestinal cells targeting are two main strategies to improve insulin oral delivery efficiency. However, few studies are available regarding the effectiveness of combining these two strategies into one nano-delivery system. For this objective, the folic acid (FA) decorated virus-mimicking nanoparticles were designed and influence of FA graft ratio on the *in vitro* and *in vivo* properties of insulin loaded nanoparticles was studied systemically. Firstly, using folic acid as active ligand, different folic acid grafted chitosan copolymers (FA-CS) were synthesized and characterized. Thereafter, using insulin-loaded poly(n-butylcyanoacrylate) nanoparticles as the core, virus-mimicking nanoparticles were fabricated by coating of positively charged FA-CS copolymer and negatively charged hyaluronic acid. Irrespective of the FA graft ratio, all the nanoparticles showed good stability, similar insulin release in the gastrointestinal fluid, excellent and similar penetration in mucus. The nanoparticles permeability in intestine was FA graft ratio and segment dependent, with FA graft ratio at/over 12.51% presenting better effect in the order of duodenum > jejunum \approx ileum. Both mechanism studies and confocal microscopy observation demonstrated FA-mediated process was involved in the transport of FA decorated nanoparticles. *In vivo* studies revealed hypoglycemic effect of the nanoparticles was FA graft ratio dependent, a saturation phenomenon was observed when FA graft ratio was at/over 12.51%. In conclusion, folic acid decorated virus-mimicking nanoparticles presented improved insulin absorption, implying combining mucus penetration and active transcellular transport is an effective way to promote oral insulin absorption, while the modification ratio of active ligand needs optimization.

1. Introduction

Biological drugs, such as peptides/proteins, are highly attractive in modern medicine because of their high potency and specificity. According to the F&D report (2019), the global biomedical market reached \$261.8 billion in 2018 and will continue to grow at an annual-growth rate of 11.8% over the next decade. However, due to the low stability and poor absorption, biological drugs are mainly administered by injection in clinic. Therefore, in order to expand their application, tremendous research and development have been carried out to develop non-invasive routes for systemic delivery of biological drugs, including oral, nasal, inhalation, buccal and transdermal routes (Anselmo et al., 2019). Especially, as the most preferred and patient-friendly alternative method to injection, oral route has attracted researchers interest for a long time (Liu et al., 2017; Eilleia et al., 2018). More interestingly, oral insulin therapy can not only improve patients compliance and reduce the side effects, but also simulate the physiological secretion of insulin

and correct the defect of glucose metabolism caused by peripheral delivery (Arbit, 2004).

It is known that mucus and the underlying intestinal cells are two main obstacles for oral insulin delivery (Liu et al., 2017). Many viruses, which are characterized by small particle size, densely coated with negative and positive charges creating a net-neutral and highly hydrophilic surface, can diffuse in mucus as fast as that in water (Lai et al., 2009). Inspired by the features of viruses, the virus-mimicking nanoparticles were developed by our group (Zhang et al., 2018; Liu et al., 2019b) to overcome the mucus barrier of oral insulin delivery, which showed an excellent penetration in the porcine mucus. However, due to lack of specific transport pathway, the uptake of virus-mimicking nanoparticles in epithelial cells was restricted, limiting the oral insulin delivery efficiency. It is reported that nanoparticles appended with different targeting ligands such as lectin, CSK peptide and Vit B₁₂ were a promising strategy to improve the intestinal absorption of insulin by interacting with the receptors on the intestinal cells membrane (Kaklotar

^{*} Corresponding author at: School of Pharmacy, Shenyang Pharmaceutical University, 103 Wenhua Road, 110016 Shenyang, China.

E-mail address: maoshirui@sypu.edu.cn (S. Mao).

<https://doi.org/10.1016/j.ijpharm.2021.120297>

Received 30 September 2020; Received in revised form 30 December 2020; Accepted 15 January 2021

Available online 26 January 2021

0378-5173/© 2021 Elsevier B.V. All rights reserved.

et al., 2016). Folic acid (FA), whose transport carrier is widely distributed across the gastrointestinal tract (GIT), was frequently used as a target ligand to promote nanoparticles enterocyte endocytosis (El Leithy et al., 2019; Xie et al., 2018; Xu et al., 2017). However, to the best of our knowledge, there are few studies on the effect of FA graft ratio on the intestinal absorption of drug-loaded nanoparticles. Moreover, the mucus presented over the gastrointestinal tract might compromise the efficiency of FA decorated nanoparticles. Therefore, in order to overcome the mucus barrier and investigate the absorption enhancing effect of FA targeting ligand on insulin loaded nanoparticles, virus-mimicking nanoparticles with different FA graft ratios were designed herein. It is assumed enhanced mucus-penetration in combination with ligand targeting nanoparticles might be more effective in enhancing oral insulin delivery.

To test this hypothesis, first of all, the core of insulin-loaded PBCA nanoparticles (Ins/PBCA NPs) was prepared by the self-polymerization of butylcyanoacrylate (BCA) in aqueous system (Cheng et al., 2020), which can not only provide good protection to its cargo, but also show pH-responsive release characteristics in the gastrointestinal fluids (Graf et al., 2009). Thereafter, folic acid-modified chitosan (FA-CS) with different modification degrees were synthesized and coated on the NPs surface to enhance ligand targeting, and negatively charged hyaluronic acid (HA) was further added to achieve virus-mimicking shell for enhanced mucus penetration. Influence of FA-CS graft ratio on the properties and stability of the nanoparticles, *in vitro* insulin release, mucus penetration and permeability of the nanoparticles in the intestine, and *in vivo* therapeutic effect were investigated systemically.

2. Material and methods

2.1. Material

Porcine insulin was purchased from Wanbang Biochemical Pharmaceutical Company. N-butylcyanoacrylate was supplied by Beijing Compant Medical Devices Co., Ltd. Poloxamer 407 (F127) was a gift from BASF. Sodium dodecyl sulfate (SDS) was obtained from Beijing Biotopped Technology Co., Ltd. Folic acid was purchased from Sigma. Carbodiimide (EDC) and N-hydroxy-succinamide (NHS) were from Shanghai Common Chemical Science and Technology Co., Ltd. Chitosan (100 kDa, DD \geq 85%) was from Jinan Haidebei marine bioengineering Co., Ltd. Hyaluronic acid (200 kDa) was from Bloomage Biotechnology Co., Ltd. Tris, Pepsin (>3000 U/mg), Trypsin (>250U/mg), Cy5-NHS, and DAPI solution were all from Dalian Meilun Biotechnology Co., Ltd.

2.2. Synthesis and characterization of folic acid-chitosan (FA-CS) copolymer

Firstly, FA, EDC and NHS (1:1.5:1.5, molar ratio) were dissolved in DMSO and stirred at 30 °C for 3 h in dark. Secondly, 100 mg CS was dissolved in 0.25% acetic acid (2 mg/mL, pH 6.0), then the activated FA solution was slowly dropped to the CS solution and stirred at 30 °C for 24 h in dark. Thereafter, the solution was centrifuged at 10,000 rpm for 10 min and the supernatant was adjusted to pH 9.0 with NaOH solution. Then, the precipitate was collected, redissolved in acetic acid solution and centrifuged at 10,000 rpm for 10 min. At last, the supernatant was dialyzed against pure water for 72 h (MWCO 8–12 K), and FA-CS was obtained after freeze-drying for 24 h at -40 °C (Li et al., 2016; Yang et al., 2014).

In order to identify the successful synthesis of FA-CS, its chemical structure was analyzed by FTIR. Briefly, the powders were compressed into disks with KBr, and scanned from 4000 to 400 cm^{-1} at resolution of 1 cm^{-1} using the spectrometer (IFS 55, Bruker). Moreover, the synthesized FA-CS was characterized by ^1H NMR. Firstly, FA was dissolved in deuterated DMSO while CS and FA-CS were dissolved in $\text{D}_2\text{O}/\text{TFA}$ (2:1, v/v). Then, the samples were analyzed by ^1H NMR at 600 MHz (AV-600, Bruker).

Moreover, UV–Vis spectrophotometer method was used to measure the content of FA in the FA-CS copolymers (Li et al., 2016). Firstly, FA-CS was dissolved in 0.25% acetic acid, then its absorbance was measured at 350 nm using UV–Vis spectrophotometer (UV 2000, Unico). And the FA content in FA-CS was obtained by reference to the FA standard calibration curve ($A = 0.015C + 0.0034$, $R^2 = 0.997$). The coupling ratio of FA was calculated by the following equation:

$$\text{CR}(\%) = \frac{W_{\text{FA}}}{W_{\text{FA-CS}} - W_{\text{FA}}} \times 100 \quad (1)$$

where W_{FA} represents the amount of FA in the FA-CS copolymer and $W_{\text{FA-CS}}$ represents the total amount of FA-CS copolymer.

2.3. Preparation and characterization of folic acid decorated nanoparticles

Insulin-loaded PBCA nanoparticles (Ins/PBCA NPs) was prepared as described previously (Cheng et al., 2020). Briefly, 20 μL BCA was dispersed in 2.0 mL HCl solution (pH 2.0) containing F127 and SDS. And the Ins/PBCA NPs were obtained by dropping insulin solution dissolved in HCl/Tris solution (1 mg/mL, pH 7.6) to the BCA solution (2/1, v/v) and stirring for 30 min at room temperature. Secondly, Ins/PBCA NPs was dropped to FA-CS solution (0.25% acetic acid, 0.6 mg/mL) in a volume ratio of 2:1 and stirred for 30 min to fabricate Ins/PBCA/FACS NPs. At last, Ins/PBCA/FACS/HA NPs was prepared by adding Ins/PBCA/FACS NPs to HA water solution (2.0 mg/mL) in a volume ratio of 2:1 and agitated for 30 min at room temperature.

The average particle size and zeta potential of the nanoparticles were analyzed using dynamic light scattering (DLS, NANO ZS90, Malvern) at 25 °C with a scattering angel of 90°. The entrapment efficiency (EE) of insulin in the nanoparticles was determined by measuring the amount of free insulin in the supernatant (15,000 rpm, 30 min) using high performance liquid chromatography (HPLC, Agilent 1100) method (Cheng et al., 2020), and EE was calculated by the following equation:

$$\text{EE}(\%) = \frac{\text{Total amount of insulin added} - \text{free insulin in supernatant}}{\text{Total amount of insulin added}} \times 100 \quad (2)$$

Then, the precipitate (15,000 rpm, 30 min) was collected and freeze dried for 24 h at -40 °C, and the loading capacity of insulin was calculated by the following equation:

$$\text{LC}(\%) = W_{\text{Insulin}}/W_{\text{NPs}} * 100 \quad (3)$$

where W_{Insulin} represents the amount of insulin wrapped in the nanoparticles and W_{NPs} represents the weight of nanoparticles.

Moreover, in order to identify the interaction between Ins/PBCA NPs and the coating layers, the prepared nanoparticles were freeze dried for 24 h at -40 °C and the obtained powders were analyzed by FTIR as described above.

2.4. Stability of folic acid decorated nanoparticles

Firstly, dilution stability of the nanoparticles in simulated gastric fluid (SGF, pH 1.2 HCl) and simulated intestinal fluid (SIF, pH 6.8 PBS) was investigated using DLS method. In brief, 200 μL nanoparticles solution was added to SGF and SIF respectively, and incubated at 37 °C/80 rpm for 4 h (SGF) and 9 h (SIF). And the particle size changes of nanoparticles were monitored by DLS at 37 °C.

Secondly, enzymatic stability of insulin in the nanoparticles was evaluated. Briefly, the nanoparticles solution (Insulin 118.5 μg) was added to 800 μL pepsin solution (pH 1.2 HCl, 9 IU/mL) and trypsin solution (pH 6.8 PBS, 375 IU/mL), respectively, and incubated at 37 °C/80 rpm. At the set time points, the samples were withdrawn, cold 0.1 N NaOH solution (pepsin) or HCl solution (trypsin) was added to stop the enzymatic reaction, and the nanoparticles were dissolved by methanol.

Then, the remaining insulin content was analyzed using HPLC after centrifugation (15,000 rpm, 30 min).

2.5. *In vitro* release of insulin from folic acid decorated nanoparticles

The release amount of insulin from the nanoparticles was determined by centrifugation method (Liu et al., 2019a). In brief, the nanoparticles solution (Insulin: 118.5 µg) was added to 800 µL SGF, SIF and pH 7.4 PBS, respectively, and incubated at 37 °C/80 rpm. At set time points, the samples were taken out and centrifuged for 30 min at 15,000 rpm. And the content of insulin in the supernatant was analyzed by HPLC. Herein, similar factor (f_2) was used to compare the release difference between nanoparticles:

$$f_2 = 50 \times \log \left\{ 1 + (1/n) \sum_{i=1}^n (R_i - T_i)^{-0.5} \times 100 \right\} \quad (4)$$

where n represents the number of time points, T_i is the release amount of the sample at different time points and R_i is the release amount of the reference at the corresponding time points. And the difference is considered significant if $f_2 < 50$.

2.6. Penetration of folic acid decorated nanoparticles in mucus

In the study, all the animal experiments followed the principle of Laboratory Animal Care and were approved by Ethics Committee of Shenyang Pharmaceutical University. The penetration of nanoparticles in mucus was evaluated as described previously (Zhang et al., 2018). Firstly, the mucus was collected from porcine intestine and Cy5 labeled insulin was synthesized. Secondly, the nanoparticles were prepared using Cy5-insulin as described above, added to mucus, mixed evenly and incubated for 10 min at 37 °C/80 rpm. At last the samples were centrifuged for 10 min at 2000 rpm and fluorescence intensity of the supernatant was measured by microplate reader (SpectraMax® M3, Molecular Devices Corporation) at excitation: 600 nm, emission: 665 nm. And penetration percentage of the nanoparticles in mucus was determined by the ratio of its fluorescence intensity in the supernatant and original nanoparticles.

2.7. Permeability of folic acid decorated nanoparticles across rat intestine

Herein, the permeability of nanoparticles across rat intestine was evaluated using ex-vivo method (Zhang et al., 2018). Firstly, Wistar rats (6–8 weeks) were executed by cervical vertebrae and their intestines were excised. Then 300 µL Cy5-labeled nanoparticles were injected into the intestinal segments with both ends sealed (~4 cm), and incubated in 10 mL Krebs-Ringer solution at 37 °C/80 rpm. At indicated time points, 200 µL sample was collected from the accept chamber and equivalent Krebs-Ringer solution was compensated. Fluorescence intensity of the collected samples was recorded by microplate reader at excitation 600 nm, emission 665 nm, and the apparent permeability coefficient (Papp) of insulin across intestine was calculated as follows:

$$P_{app} = \frac{dQ}{dt} \frac{1}{A \cdot C_0} \quad (5)$$

where dQ/dt means the permeability rate of Cy5-insulin, A means the surface area of intestine and C_0 means Cy5-insulin initial concentration in the donor chamber.

Furthermore, the uptake mechanisms of FA decorated nanoparticles in intestine were studied. In brief, the labeled nanoparticles were loaded into duodenum and incubated in Krebs-Ringer solution containing different absorption inhibitors, including folic acid (40 mg/mL), indomethacin (20 µg/mL), chlorpromazine (10 µg/mL) and colchicine (5 µg/mL) at 37 °C/80 rpm. In addition, the duodenum was also incubated at low temperature (4 °C) without inhibitors while the other procedures were the same as described above.

2.8. Observation of folic acid decorated nanoparticles uptake in enterocyte

In this study, uptake of the nanoparticles in enterocyte was intuitively observed by confocal laser scanning microscopy (CLSM, LSM 710, Zeiss). Firstly, the fasted rats (6–8 weeks) were anesthetized with chloral hydrate by intraperitoneal injection. Then, a small incision was made in rats abdomen, both ends of the different intestinal segments (~4 cm) were sealed after the Cy5 labeled nanoparticles solution (300 µL) being injected. One hour later, the rats were sacrificed and their intestinal segments were excised with gently rinsing by 5 mL saline. Then, the intestinal segments were fixed for 2 h in 4% paraformaldehyde and dehydrated for 12 h in 30% sucrose. Thereafter, the intestinal loops were embedded into O.C.T compound and frozen for cutting with Cryotome (SLEE medical GmbH, D-55136 Mainz). At last, the epithelial nucleus was labeled by DAPI solution (10 µg/mL) and the intestinal slices were observed by CLSM at EX/EM 405/497 nm for DAPI and EX/EM 633/700 nm for Cy5-Insulin.

2.9. Hypoglycemic effect

The hypoglycemic effect of FA decorated virus-mimicking nanoparticles was evaluated in diabetic rats. Firstly, the diabetic rats were induced with alloxan in Wistar rats (200 ± 20 g) (Cheng et al., 2020). Secondly, the diabetic rats were fasted overnight but with free access to water and then administered by the following formulations ($n = 4$ for each group): insulin solution by oral (50 IU/kg), insulin solution by subcutaneous injection (5 IU/kg), Ins/PBCA/CS/HA and Ins/PBCA/FACS/HA NPs solution by oral (50 IU/kg). At last, the blood glucose level of diabetic rats was monitored with blood glucose meter (JPS-6, Beijing Yicheng) as described previously (Liu et al., 2019a). And the pharmacological availability (PA) was calculated according to the following equation:

$$PA(\%) = \frac{AAC_{p.o.}/Dose_{p.o.}}{AAC_{s.c.}/Dose_{s.c.}} \times 100 \quad (6)$$

where AAC is the area above the blood glucose level curve, s.c. means subcutaneous injection, p.o. means oral administration.

2.10. Toxicity studies

In order to investigate the *in vivo* safety of nano-delivery system, the gastrointestinal irritation study was carried out in healthy Wistar rats (200 ± 20 g). Firstly, the rats were divided into saline group and nanoparticles group. Then, the saline and nanoparticles groups were daily given physiological saline solution (3.0 mL/Kg) and Ins/PBCA/FA_{12.51}-CS/HA NPs solution (50 IU/Kg) by gavage, respectively. After 7 days, the rats were sacrificed and the different gastrointestinal segments (stomach, duodenum, jejunum and ileum) were excised and gently washed with physiological saline solution, fixed in paraformaldehyde (4%, w/v) and cut into 5 µm thick paraffin sections. At last, the paraffin sections were stained by H&E (hematoxylin and eosin) and observed using stereomicroscope.

2.11. Statistical analysis

The experimental data were expressed by mean value ± standard deviation ($n \geq 3$). And the group data were analyzed by two tail student's *t*-test and one-way ANOVA with GraphPad Prism 6 at the probability level of 0.05.

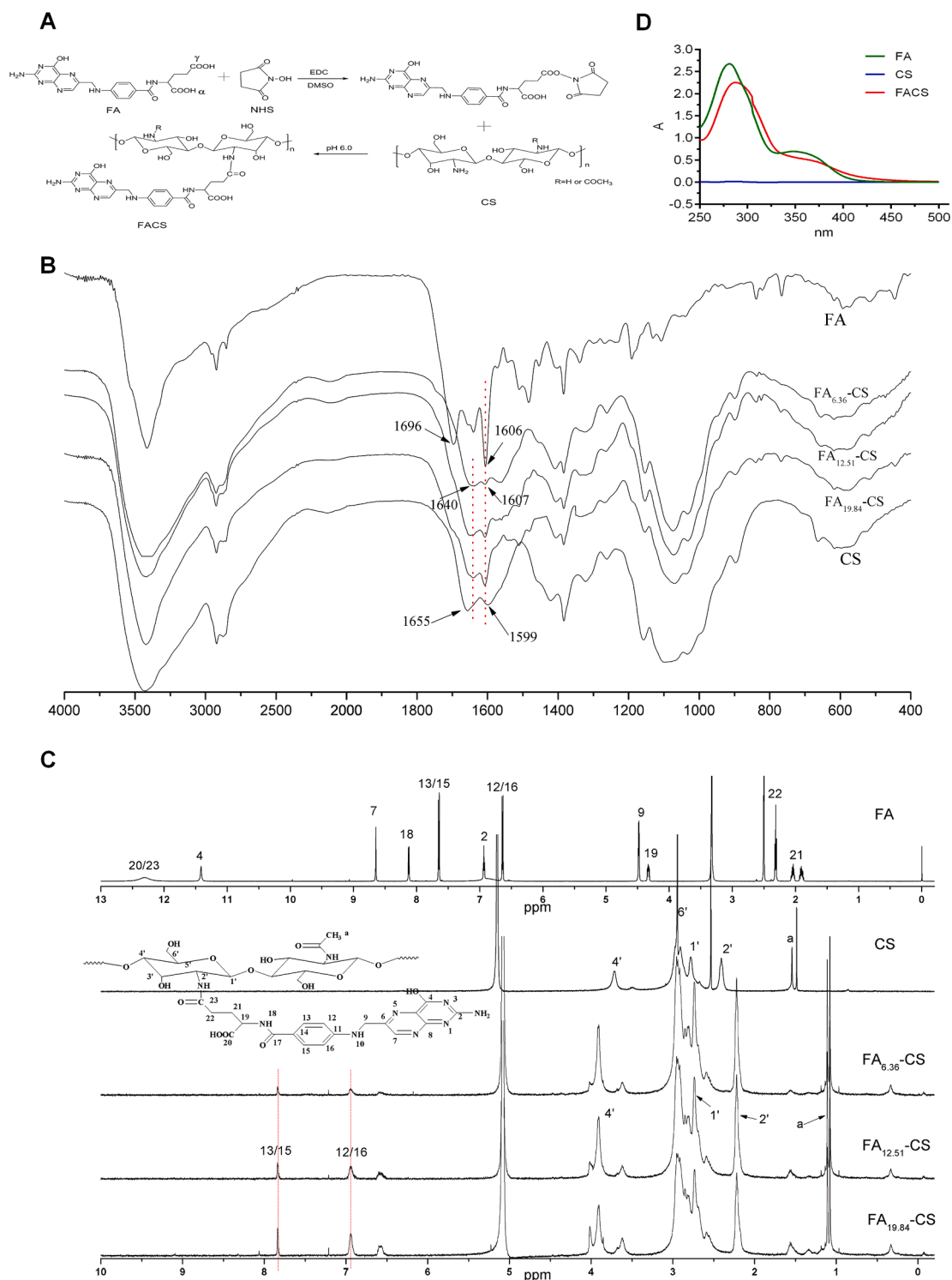


Fig. 1. (A) Synthesis scheme of folic acid-chitosan (FACS) copolymers, (B) FTIR spectra of CS, FA and FA-CS copolymers, (C) ^1H NMR spectrum of CS, FA and FA-CS copolymers, (D) UV curve of FA, CS and FA_{12.51}-CS copolymers.

3. Results and discussion

3.1. Synthesis and characterization of folic acid-chitosan copolymers

The copolymers of folic acid grafted chitosan (FA-CS) was synthesized by the reaction between the carboxyl group of FA and the amino groups of CS via the formation of amide bond. As shown in Fig. 1(A), the γ -COOH of FA, which has higher reactivity than α -COOH (Zhang et al., 2007), was firstly activated by NHS/EDC reaction, then the activated FA

ester reacted with the primary amino groups of CS and the FA-CS copolymers were obtained. To investigate the influence of FA graft ratio on the *in vitro* and *in vivo* properties of the nanoparticles, FA-CS copolymers with different coupling ratios, which were 6.36%, 12.51% and 19.84%, respectively, were synthesized herein by adjusting FA and chitosan molar ratio. Firstly, FTIR was used to investigate the structural characteristics of FA-CS copolymers (Fig. 1B). It is known the absorption peak of FA at 1696 cm^{-1} and 1606 cm^{-1} belong to the vibration of carboxyl and pethidine ring amino groups, respectively. The absorption peak of

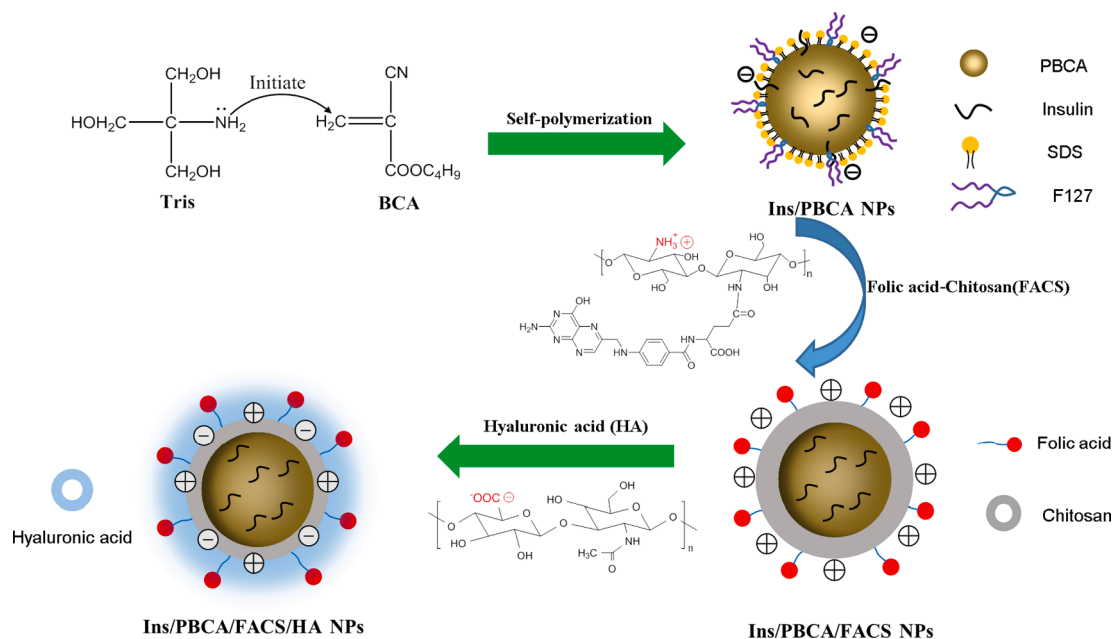


Fig. 2. The preparation mechanism and structure of Ins/PBCA, Ins/PBCA/FACS and Ins/PBCA/FACS/HA NPs.

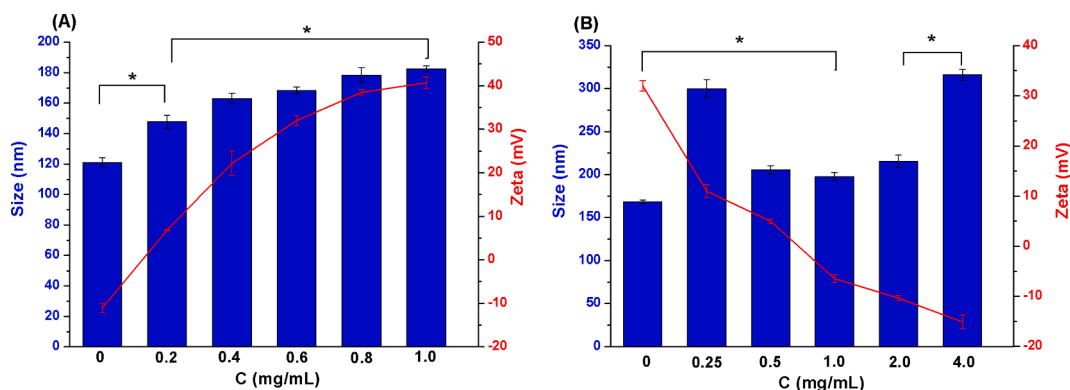


Fig. 3. (A) Influence of FA_{6,36}-CS concentration on Ins/PBCA/FA_{6,36}-CS NPs characteristics; (B) HA concentration on Ins/PBCA/FA_{6,36}-CS/HA NPs characteristics. Symbols indicate statistically significant differences (**p* < 0.05).

Table 1

The characteristics of insulin-loaded PBCA nanoparticles.

Nanoparticles	Graft ratio/%	Size/nm	Zeta/mV	EE/%	LC/%
Ins/PBCA	/	120.90 ± 3.18	-11.13 ± 1.00	99.76 ± 0.10	30.11 ± 1.65
Ins/PBCA/FACS	CS	150.75 ± 4.32*	32.85 ± 1.35	99.87 ± 0.11	22.54 ± 1.29
	FA _{6,36} -CS	168.37 ± 2.20 [#]	32.00 ± 1.06	99.91 ± 0.09	21.52 ± 0.86
	FA _{12,51} -CS	184.05 ± 6.55	31.15 ± 1.20	99.90 ± 0.06	21.95 ± 0.94
	FA _{19,84} -CS	200.25 ± 8.84	30.25 ± 1.89	99.89 ± 0.10	21.69 ± 0.59
	CS	197.13 ± 6.42	-10.25 ± 0.20	99.91 ± 0.02	16.43 ± 0.42
Ins/PBCA/FACS/HA	FA _{6,36} -CS	215.45 ± 7.22	-10.37 ± 0.51	99.89 ± 0.01	16.67 ± 0.16
	FA _{12,51} -CS	241.15 ± 7.99	-10.60 ± 0.21	99.87 ± 0.01	16.73 ± 0.33
	CS	275.95 ± 7.00	-11.70 ± 0.42	99.87 ± 0.02	16.46 ± 0.23
	FA _{19,84} -CS	275.95 ± 7.00	-11.70 ± 0.42	99.87 ± 0.02	16.46 ± 0.23
	CS	7.00	0.42	0.02	0.23

Note: Symbols indicate statistically significant differences (*p* < 0.05), (*) compared to Ins/PBCA NPs, (#) compared to Ins/PBCA/CS NPs.

CS at 1655 cm⁻¹ and 1599 cm⁻¹ correspond to the vibration of amide I (C=O stretch) and amide II (NH blending) groups. The spectrum of synthesized FA-CS copolymers displayed that the peak of FA at 1696 cm⁻¹ disappeared and a new peak corresponding to C=O bond vibration of -CONH- appeared at 1640 cm⁻¹. Moreover, the peaks of CS at 1655 cm⁻¹ and 1599 cm⁻¹ were shifted to 1640 cm⁻¹ and 1607 cm⁻¹, respectively, indicating the successful synthesis of FA-CS copolymers (Li et al., 2016). It can be found the intensity of FA-CS peak at 1607 cm⁻¹ increased with the increase of FA amount, suggesting the increase of FA-CS graft ratio. Then, the structural characteristics of FA-CS copolymers were confirmed using ¹H NMR. As shown in Fig. 1(C), the ¹H NMR spectrum of FA-CS copolymers contained a series of peaks originating from both FA and CS. The signal at 7.8 and 6.9 ppm correspond to the protons of H-13/15 and H-12/16 of FA, respectively, and the signal at 3.6, 2.7, 2.2 and 1.1 ppm correspond to the protons of H-4', H-1', H-2' and H-a of CS, respectively (Wang et al., 2014), further confirming FA was successfully grafted onto CS. Moreover, the increase of FA-CS copolymers peak intensity at H-13/15 and H-12/16 also indicated FA-CS grafting ratio increased with the increase of FA amount. Moreover, UV spectrum was used to identify the characteristic of FA-CS copolymers. As shown in Fig. 1(D), in the range of 250–500 nm, CS didn't show any UV absorption, and FA showed maximum absorption at 281 and 350 nm

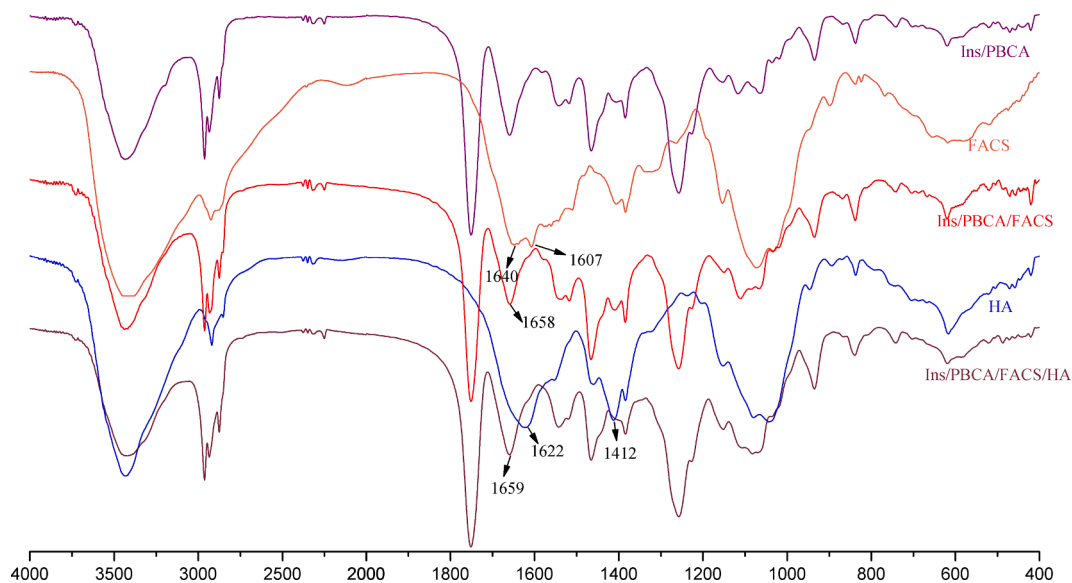


Fig. 4. FTIR spectra of Ins/PBCA NPs, folic acid-chitosan (FA_{12.51}-CS) copolymers, Ins/PBCA/FACS NPs, hyaluronic acid (HA) and Ins/PBCA/FACS/HA NPs.

while the spectrum of FA-CS copolymers shifted to higher wavelength and the second absorption peak was less obvious relative to the FA spectrum, suggesting the successful synthesis of FA-CS copolymers.

3.2. Influence of FA-CS graft ratio on the properties of nanoparticles

Herein, insulin was firstly wrapped in PBCA nanoparticles (Ins/PBCA NPs) with BCA self-polymerization by the stimulation of Tris (Cheng et al., 2020) (Fig. 2). And in the process of preparation, SDS and F127

were introduced into the system to improve the dispersion of BCA and physical stability of the nanoparticles (Dong et al., 2018). As shown in Fig. 3(A), the Ins/PBCA NPs were slightly negatively charged. After adding to FACS solution, surface charge of the nanoparticles changed from negative to positive and the particle size increased significantly ($p < 0.05$), indicating the successful coating of FACS on Ins/PBCA NPs. And particle size and surface charge of the nanoparticles increased gradually with the increase of FACS concentration, indicating the increase of coating thickness. As it is generally recognized that the nanoparticles

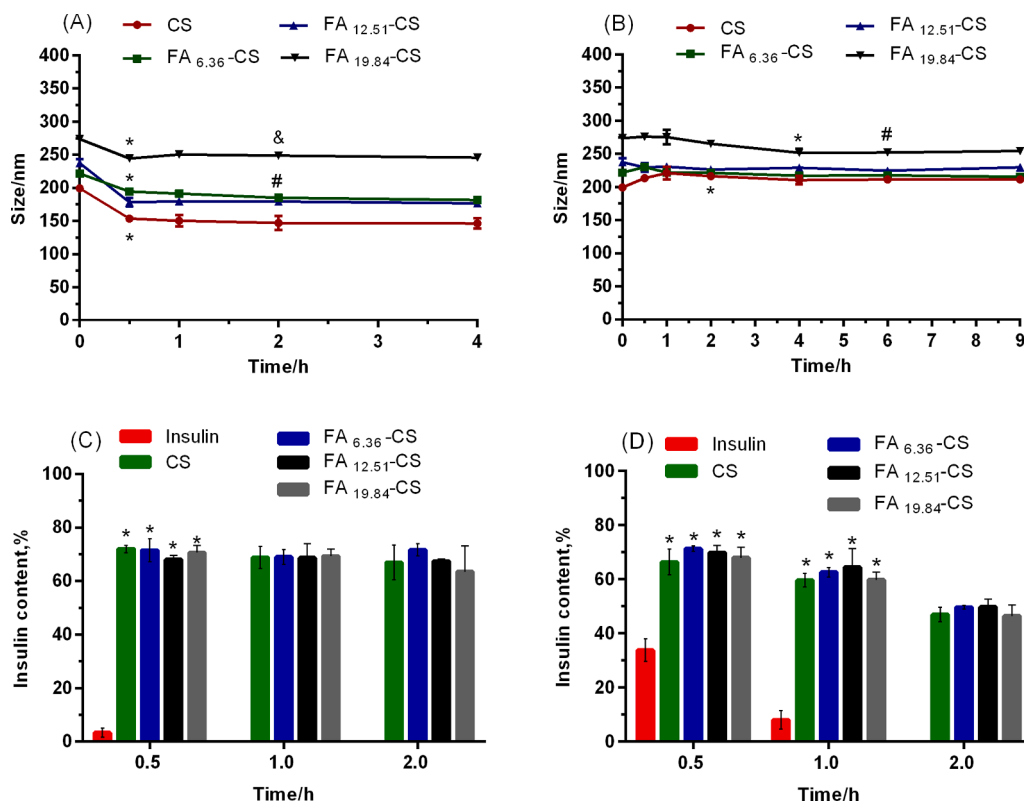


Fig. 5. The size change of Ins/PBCA/FACS/HA NPs versus time (A) in pH 1.2 HCl, (*) compared to initial, (#) compared to CS group, (&) compared to FA_{12.51}-CS group; (B) in pH 6.8 PBS (0.05 M), (*) compared to initial, (#) compared to CS group. Symbols indicate statistically significant differences (* $p < 0.05$). Enzyme stability of Ins/PBCA/FACS/HA NPs (C) in pepsin, (D) in trypsin. (*) compared to insulin.

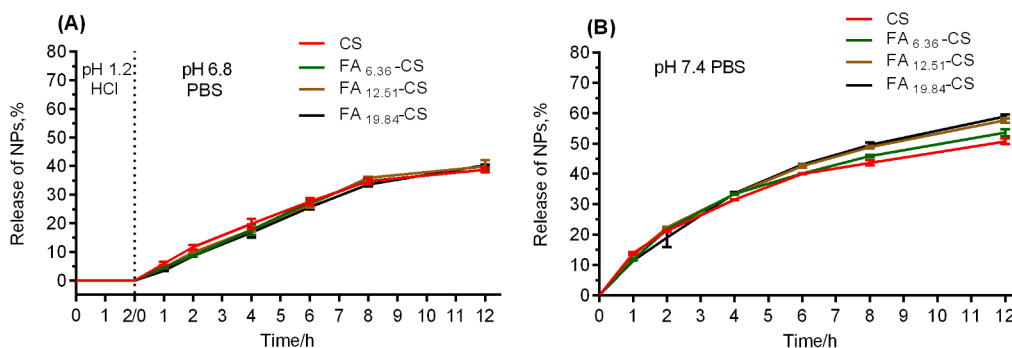


Fig. 6. Insulin release from Ins/PBCA/FACS/HA NPs in pH1.2 HCl, pH6.8 PBS and pH7.4 PBS (0.05 M).

with surface charge greater than 25 mV are more stable, 0.6 mg/mL FACS was used to prepare the Ins/PBCA/FACS NPs. As shown in Table 1, with the increase of FA-CS graft ratio, the particle size of Ins/PBCA/FACS NPs increased while its surface charge decreased slightly. Since the primary amino groups of CS decreased with the increase of FA graft ratio, the electrostatic interaction between FACS and Ins/PBCA NPs might be weakened, probably resulting in a relatively loose structure of Ins/PBCA/FACS NPs (Zhang et al., 2018) and thus a slightly decrease of its surface charge (Agrawal et al., 2015).

It is known mucus present on the intestinal epithelial cells greatly impeded the transport of nanoparticles (Pearson et al., 2016), which might discount the contribution of ligand based epithelial cells targeting. Cone et al. found many viruses with dense coating of positively and negatively charged groups could diffuse in mucus as quick as that in water (Olmsted et al., 2001). Thus, in order to overcome the mucus barrier, the virus-mimicking nanoparticles were fabricated with the coating of hyaluronic acid (HA) on Ins/PBCA/FACS NPs (Fig. 2). Firstly, taking FA_{6.36}-CS coated nanoparticles as an example, influence of HA concentration on the properties of the nanoparticles was investigated. As shown in Fig. 3(B), with the increase of HA concentration, surface charge of the nanoparticles decreased, which changed from positive to negative when HA concentration was increased to 1 mg/mL. Moreover, particle size of the nanoparticles increased significantly ($p < 0.05$) with HA addition, indicating successful coating of HA on Ins/PBCA/FACS NPs. It was noted particle size of the nanoparticles increased sharply with 0.25 mg/mL HA addition, indicating structure of the nanoparticles was not compacted contributed to the weak electrostatic interaction (Zhang et al., 2018). And no particle size difference was found in the HA concentration range of 0.5–2 mg/ml while it increased significantly when HA concentration was increased to 4.0 mg/ml, indicating increase of coating thickness. Moreover, probably due to the nearly net-neutral surface charge and thin coating layer, aggregation of nanoparticles was observed after 48 h when HA concentration was less than 1.0 mg/mL. Therefore, in order to simulate the surface properties of virus and meanwhile guarantee stability of the nanoparticles, 2.0 mg/mL HA was selected for coating in further study.

As revealed in Table 1, after HA coating, surface charge of all the Ins/PBCA/FACS/HA NPs was reversed and their particle size increased significantly in a FA-CS graft ratio dependent manner, indicating successful coating of HA on the Ins/PBCA/FACS NPs. The entrapment efficiency (EE) of insulin in all the nanoparticles was more than 99%, indicating the coating process and FA-CS graft ratio had no effect on the EE of insulin.

Moreover, the coating mechanism was analyzed by FTIR. As shown in Fig. 4, after coating of FACS on the Ins/PBCA NPs, the amide I (C=O stretch, 1640 cm^{-1}) absorption peak of FACS was shifted to 1658 cm^{-1} and its amide II (NH blending) absorption peak at 1607 cm^{-1} disappeared, indicating electrostatic interaction was involved in the coating process of Ins/PBCA/FACS NPs (Jin et al., 2011). For the Ins/PBCA/FACS/HA NPs, after HA coating, the asymmetric stretching peak (1622 cm^{-1}) of carboxylate anion of HA was shifted to 1659 cm^{-1} and

its symmetric stretching peak (1412 cm^{-1}) disappeared, implying HA coating layer was also formed by electrostatic interaction (Gilli et al., 1994; Li et al., 2013).

3.3. Influence of FA-CS graft ratio on the stability of nanoparticles

It is known that stability of the nanoparticles was greatly affected by the pH and enzymes in the GIT (Zhang et al., 2018). Herein, dilution stability of the Ins/PBCA/FACS/HA NPs in different pH was firstly investigated by DLS. As revealed in Fig. 5(A), in pH 1.2 HCl, particle size of the nanoparticles with different FA-CS graft ratios showed a decrease at first and remained constant for the next few hours. Compared with the unmodified nanoparticles, FA decorated nanoparticles all showed a bigger particle size in pH 1.2 medium, and the FA_{19.84}-CS decorated nanoparticles had the biggest particle size while no significant difference was found between the FA_{6.36}-CS and FA_{12.51}-CS groups. As revealed in Fig. 5(B), in pH 6.8 PBS, particle size of the CS group showed a slight increase, and no significant change in particle size was found for FA_{6.36}-CS and FA_{12.51}-CS groups while a slight decrease in particle size was observed in FA_{19.84}-CS group. Overall, the FA_{19.84}-CS decorated nanoparticles showed the largest particle size in pH 6.8 PBS while no significant difference was found among the other nanoparticles with lower FA-CS graft ratios. The particle size of Ins/PBCA/FACS/HA NPs with different FA-CS graft ratios ranged from 100 to 300 nm in pH 1.2 HCl and pH 6.8 PBS, indicating their good dilution stability in the gastrointestinal fluids.

Thereafter, pepsin and trypsin, which are two important digestive enzymes in GIT, were used to evaluate the enzyme stability of insulin in Ins/PBCA/FACS/HA NPs. As shown in Fig. 5(C), free insulin was quickly degraded by pepsin and no insulin could be detected after 1 h incubation in pepsin solution. In contrast, the stability of insulin encapsulated in nanoparticles was dramatically improved. The remained insulin content was still above 60% after 2 h incubation in pepsin solution and no significant difference was found among the different FA-CS graft ratio nanoparticles ($p > 0.05$). Similarly, as revealed in Fig. 5(D), the trypsin stability of insulin was also greatly improved by nanoparticles, and the content of insulin in nanoparticles was about 50% after 2 h incubation in trypsin solution while the content of free insulin dropped to 30% within half an hour and could not be detected after 2 h. No significant difference in insulin content was found among the different FA-CS graft ratio nanoparticles in trypsin solution ($p > 0.05$). Overall, the Ins/PBCA/FACS/HA NPs with different FA-CS graft ratios all provided good protection for insulin in GIT, which would be beneficial for clarifying the effect of FA-CS graft ratio on insulin intestinal absorption.

3.4. Influence of FA-CS graft ratio on the *in vitro* release of insulin

Herein, the *in vitro* release of insulin from Ins/PBCA/FACS/HA NPs was investigated in different pH media. As shown in Fig. 6(A), in pH 1.2 HCl, no insulin was released from nanoparticles with different FA-CS graft ratio, indicating their good stability in acid fluid. In pH 6.8 PBS,

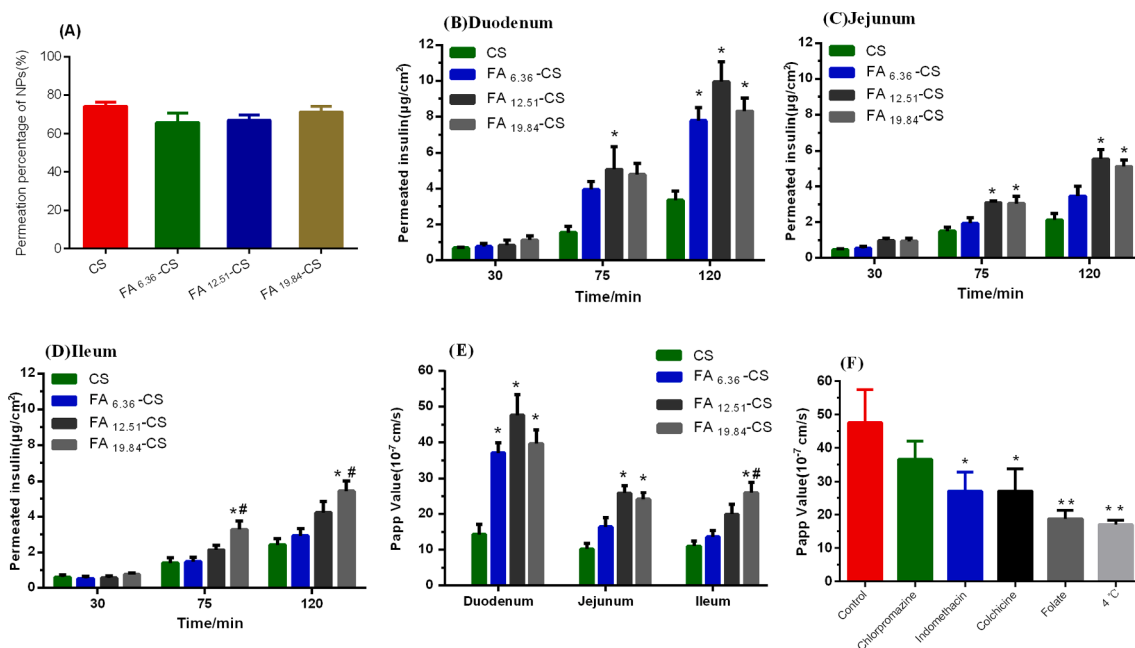


Fig. 7. (A) Penetration percentage of Ins/PBCA/FACS/HA NPs in original mucus. The accumulative amount of insulin transported through different rats' intestinal segments (B) Duodenum; (C) Jejunum; (D) Ileum; (E) Apparent permeability coefficient (Papp) of insulin in different rat intestine segments (*versus CS group, #versus FA_{6.36}-CS group); (F) Papp of insulin from Ins/PBCA/FA_{12.51}-CS/HA NPs in duodenum in presences of different uptake inhibitors (*versus control, * $p < 0.05$, ** $p < 0.01$).

insulin was continuously released from nanoparticles and no significant difference was found among the nanoparticles with different FA-CS graft ratio ($f_2 > 50$). It is known that the release behavior of drug from nanoparticles is closely related to the properties of carrier materials and their combination mode. It is reported that insulin was encapsulated in PBCA nanoparticles by the non-covalent bond (Sullivan and Birkinshaw, 2004) and the degradation rate of PBCA in alkaline fluid was very slow (Sulheim et al., 2016). Therefore, it can be speculated that the main release mechanism of insulin from Ins/PBCA/FACS/HA NPs was passive diffusion.

Moreover, the release of insulin from Ins/PBCA/FACS/HA NPs was also evaluated in physiological fluid (pH 7.4 PBS) to test the influence of pH on drug release. As shown in Fig. 6(B), consistent with that in pH 6.8 PBS, insulin was released from the nanoparticles in a sustained manner in pH 7.4 PBS and the FA-CS graft ratio had no significant effect on its release rate ($f_2 > 50$). However, a higher insulin release rate was found in pH 7.4 PBS relative to that in pH 6.8 PBS. Overall, the release of insulin from Ins/PBCA/FACS/HA NPs was pH-dependent, and insulin release was inhibited in acidic medium, and increased with the increase of pH. To the best of our knowledge, this pH respond release mode is an ideal nano-delivery system for oral biomacromolecule, which can not only improve insulin stability in stomach, but also promote its absorption in intestine and physiological fluid (Wong et al., 2017). Moreover, the similar insulin release behavior of Ins/PBCA/FACS/HA NPs with different FA-CS graft ratios in GIT provides a prerequisite for the study of their intestinal absorption.

3.5. Influence of FA-CS graft ratio on the mucus penetration of nanoparticles

Mucus, which distributes along the GIT and protects the underlying epithelial cells, is also a natural barrier for oral nano-delivery system. Nowadays, mucus-penetrating nanoparticles, which could penetrate the mucus layers deeply even to the absorption surface of intestinal cells, have been widely used to overcome the mucus barrier (Liu et al., 2015). Herein, the mucus-penetrating nanoparticles (Ins/PBCA/FACS/HA NPs) was designed by mimicking the surface properties of virus and their

penetration in porcine mucus was investigated. As shown in Fig. 7(A), the permeation percentage of Ins/PBCA/FACS/HA NPs with different FA-CS graft ratios were all more than 60% after 10 min of incubation in mucus, and no significant difference was found among them ($p > 0.05$), which was much larger than the positively charged Insulin/Chitosan NPs (5%) or negatively charged Insulin/Chitosan/Alginate NPs (22%) previously designed by our group (Zhang et al., 2018). It is known that the gastrointestinal mucus are composed of water, mucins, lipids and proteins, etc (Lai et al., 2009). And the negatively charged mucins are the main component of mucus, which are easy to capture the positively charged nanoparticles by electrostatic interaction. Meanwhile, the network formed by the long chain of mucins tend to trap the particles larger than 500 nm (Roger et al., 2010). Moreover, the hydrophobic interaction offered by mucins and lipids can hinder the penetration of hydrophobic substances. The mucus-penetrating nanoparticles designed herein was composed of hydrophobic core (Ins/PBCA) and hydrophilic coating layer (FACS/HA) with a slight negative surface charge and small particle size (< 300 nm). Furthermore, the nanoparticles showed good stability and little insulin release (10 min) in the gastrointestinal fluids (Fig. 6). Therefore, probably due to the virus-mimicking surface properties and good stability in GIT (Malhaire et al., 2016), the Ins/PBCA/FACS/HA NPs were less entrapped by mucus, resulting in their excellent penetration in mucus. Overall, the Ins/PBCA/FACS/HA NPs with different FA-CS graft ratios showed excellent and similar permeability in mucus, which is beneficial for clarifying the effect of FA-CS graft ratio on insulin intestinal absorption.

3.6. Influence of FA-CS graft ratio on the permeability of nanoparticles in intestine

In order to investigate the influence of FA-CS graft ratios on insulin intestinal absorption, the permeability of Ins/PBCA/FACS/HA NPs in different intestine segments were studied by *ex-vivo* method and shown in Fig. 7(B-D). It was demonstrated that the absorption of insulin increased over time in duodenum, and compared with the unmodified nanoparticles (CS group), the FA-CS decorated nanoparticles showed significantly enhanced insulin absorption in 75 min and 120 min ($p < 0.05$)

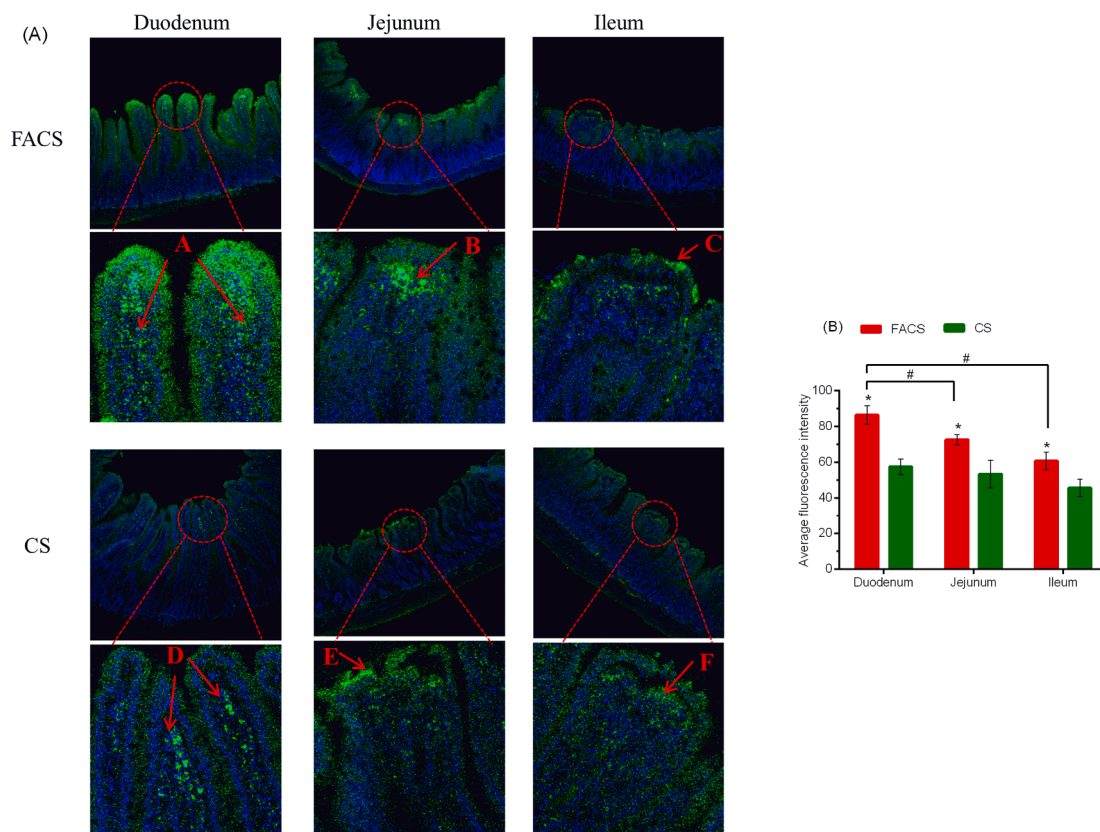


Fig. 8. Observation of Ins/PBCA/CS/HA and Ins/PBCA/FA_{12.51}-CS/HA NPs on microvilli absorption (1 h). (A) Confocal images; (B) Average fluorescence intensity. The cells were stained by DAPI (Blue). Symbols indicate statistically significant differences ($p < 0.05$, *versus CS group, #versus indicated group).

while no significant difference was found in 30 min, indicating FA carriers participated in the intestinal transport of FA-CS decorated nanoparticles and the process was time dependent. Moreover, in duodenum, no significant difference was found in insulin absorption among the FA_{6.36}-CS, FA_{12.51}-CS and FA_{19.84}-CS groups ($p > 0.05$). Compared to that in duodenum, insulin absorption in jejunum was remarkably decreased and the influence of FA graft ratio was more apparent. It was noted that in jejunum, no significant difference in insulin absorption was found between the CS and FA_{6.36}-CS groups ($p > 0.05$), while statistically enhanced insulin absorption was observed in FA_{12.51}-CS and FA_{19.84}-CS groups, and no difference was found between these two groups ($p > 0.05$). And in ileum, the FA_{19.84}-CS group showed more insulin absorption than that of the CS or FA_{6.36}-CS group ($p < 0.05$) while no significant difference between the FA_{12.51}-CS and FA_{19.84}-CS groups was found. Moreover, the apparent permeability coefficient (Papp) of insulin was further calculated to evaluate the effect of FA-CS graft ratio on the intestinal absorption of insulin. As revealed in Fig. 7 (E), the FA-CS decorated nanoparticles showed the best insulin absorption in duodenum, which was 2.6- to 3.3-fold higher than that of unmodified nanoparticles. And in jejunum/ileum, the nanoparticles with higher FA-CS graft ratios (FA_{12.51}-CS, FA_{19.84}-CS) showed more insulin absorption than that of CS group while no significant difference was found between the FA_{12.51}-CS and FA_{19.84}-CS groups ($p > 0.05$). It is reported that the reduced folate carrier (RFC) and proton-coupled folate transporter/hem carrier protein 1 (PCFT/HCP1) are two main transporters mediating folic acid intestinal absorption, and the RFC is widely distributed across the GIT while PCFT/HCP1 mRNA is particularly expressed in the duodenum and to a less extent in jejunum (Qiu et al., 2006). Furthermore, it is known the duodenum is characterized by a thin mucus layer, which is beneficial for nanoparticles penetration (Ensign et al., 2012). Therefore, probably due to the thin mucus and specialized carrier, the FA-CS decorated nanoparticles were easier to pass through

the mucus layer to intestinal epithelial cells and interacted with the FA receptors, resulting in their better absorption in duodenum.

Moreover, FA-CS graft ratio dependent drug absorption enhancing effect can probably be explained by the fact that herein hyaluronic acid (HA) was used to improve nanoparticles penetration in mucus by coating on the surface of Ins/PBCA/FACS NPs. The HA coating layer might produce a shielding effect to the FA targeting ligand. In addition, the expression of PCFT/HCP1 mRNA was less in jejunum. Therefore, probably due to the shielding effect of HA and reducing of FA receptors, few ligands of the FA_{6.36}-CS decorated nanoparticles interacted with the FA receptors, resulting in limited insulin absorption improvement in jejunum. However, with the increase of FA-CS graft ratio, more FA ligands might be exposed to the surface of nanoparticles, and the FA ligand-receptor interaction might occur between the nanoparticles and intestinal cells, leading to the improvement of insulin absorption for the FA_{12.51}-CS and FA_{19.84}-CS groups in jejunum. In ileum, probably due to the limited transport efficiency of RFC (Qiu et al., 2006), the nanoparticles with high FA-CS graft ratio (FA_{19.84}-CS) was more likely to be absorbed by the FA ligand-receptor transport pathway, resulting in its best absorption in ileum. Overall, the study revealed that FA decorated nanoparticles could improve insulin intestinal uptake and the FA-CS graft ratio had a certain effect on its absorption.

To further understand the transport mechanisms of FA decorated nanoparticles in intestine, taking FA_{12.51}-CS as the targeting ligand and duodenum as the research segment, the intestinal uptake of Ins/PBCA/FACS/HA NPs in Krebs-Ringer (KR) solution containing different absorption inhibitors was studied. As shown in Fig. 7(F), in the KR solution containing oversupplied FA, the intestinal absorption of insulin was reduced by 60.57%, further verifying FA carrier-mediated process was involved in the transport of Ins/PBCA/FACS/HA NPs. And the significant decrease of insulin absorption in the colchicine and indomethacin solution ($p < 0.05$) indicated that the macropinocytosis and caveolin-

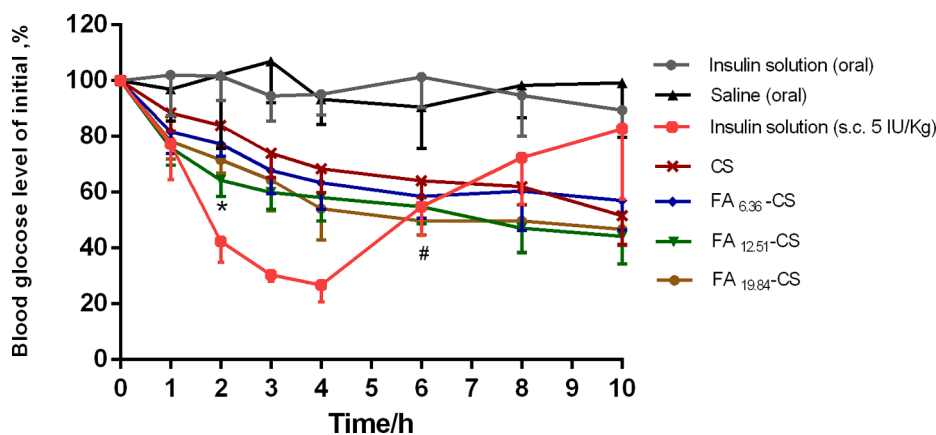


Fig. 9. Blood glucose level vs. time profiles following administration of nanoparticles in diabetic rats. Data are means \pm SD (n = 4). Symbols indicate statistically significant differences ($*p < 0.05$), (*) FA_{6.36}-CS group versus FA_{12.51}-CS group, (#) CS group versus FA_{19.84}-CS group. Note: the results of saline group and insulin solution groups were adapted from our previous study (Cheng et al., 2020).

mediated endocytosis also participated in the transport of Ins/PBCA/FACS/HA NPs in intestine. Moreover, insulin absorption was greatly reduced in low temperature (4 °C), suggesting the intestinal transport of Ins/PBCA/FACS/HA NPs also relayed on energy. In summary, multiple mechanisms were involved in the transport of Ins/PBCA/FACS/HA NPs in intestine and insulin absorption could be improved by the FA ligand-receptor targeting effect.

3.7. Observation of folic acid decorated nanoparticles uptake in enterocyte

The intestinal permeability study revealed the absorption of Ins/PBCA/FACS/HA NPs was FA graft ratio and intestinal site dependent. Herein, taking Ins/PBCA/FA_{12.51}-CS/HA NPs as an example, its uptake and penetration in intestinal microvilli was further observed by CLSM technique. As revealed in Fig. 8, compared with the unmodified nanoparticles (CS), the FA decorated nanoparticles (FACS) showed stronger fluorescence intensity in duodenum ($p < 0.05$), further demonstrated that the FA carriers participated in the transcellular transport of Ins/PBCA/FACS/HA NPs and promoted insulin intestinal uptake. Moreover, the Ins/PBCA/FACS/HA NPs showed more insulin uptake in duodenum relative to that in jejunum/ileum ($p < 0.05$), and more nanoparticles could be found in the middle and bottom of duodenum (A-C), indicating FA receptors, especially PCFT/HCP1 transporter, promoted the uptake and penetration of Ins/PBCA/FACS/HA NPs in duodenal microvilli. In jejunum, the FACS group also showed a better insulin absorption than the CS group ($p < 0.05$), and probably due to the limited expression of PCFT/HCP1 mRNA (Qiu et al., 2006), the Ins/PBCA/FACS/HA NPs had a less uptake in jejunum than that in duodenum ($p < 0.05$). Compared with the CS group, the FACS group promoted insulin uptake in ileum ($p < 0.05$). However, probably due to the thick mucus (Ensign et al., 2012) and limited RFC transport efficiency (Qiu et al., 2006), compared with the duodenum, the uptake of Ins/PBCA/FACS/HA NPs in ileum was poor ($p < 0.05$) and mainly distributed in the border of ileal microvilli. Thus, CLSM studies further verified that the intestinal absorption of insulin could be improved by the FA receptor mediated transport of Ins/PBCA/FACS/HA NPs, with the best absorption in duodenum.

3.8. Hypoglycemic effect

In vitro studies revealed the Ins/PBCA/FACS/HA NPs could improve insulin intestinal uptake by promoting its mucus penetration and transcellular transport mediated by FA carriers. And in order to evaluate the influence of FA-CS graft ratio on insulin *in vivo* absorption, the hypoglycemic effect of Ins/PBCA/FACS/HA NPs in diabetic rats was further studied. As shown in Fig. 9, after oral administration, the insulin-

Table 2

Pharmacological availability in diabetic rats given an oral insulin dose of 50 IU/kg. Data are means \pm SD (n = 4).

Nanoparticles	Administration route	Dosage (IU/kg)	AAC (%*h)	PA (%)
Insulin solution	Injection	5	422.40 \pm 62.22	100
Insulin solution	Oral	50	50.33 \pm 43.25	1.20 \pm 1.03
Ins/PBCA/CS/HA	Oral	50	296.68 \pm 54.82	7.02 \pm 1.30
Ins/PBCA/FA _{6.36} -CS/HA	Oral	50	332.90 \pm 65.05	7.88 \pm 1.54
Ins/PBCA/FA _{12.51} -CS/HA	Oral	50	414.05 \pm 65.67	9.80 \pm 1.55*
Ins/PBCA/FA _{19.84} -CS/HA	Oral	50	408.60 \pm 73.07	9.67 \pm 1.73*

Symbols indicate statistically significant differences ($p < 0.05$, * versus CS group).

Note: the results of insulin solution groups were adapted from our previous study (Cheng et al., 2020).

loaded nanoparticles all showed obvious hypoglycemic effect while the insulin solution failed to reduce the blood glucose level in diabetic rats, indicating the nanoparticles designed herein could improve insulin oral delivery efficiency. And compared with subcutaneous injection of insulin, oral insulin nanoparticles showed a mild and sustained hypoglycemic effect, and this might be able to avoid the side effect of hypoglycemia caused by subcutaneous injection. Probably due to the limited FA carriers-mediated transport, the FA_{6.36}-CS decorated nanoparticles showed comparable hypoglycemic effect relative to the CS group and no significant difference in pharmacological availability (PA) was found between them (Table 2) ($p > 0.05$). In contrast, a more obvious hypoglycemic effect was observed when FA graft ratio was increased to 12.51% (FA_{12.51}-CS) ($p < 0.05$), indicating FA carriers-mediated transport contributed to improved insulin *in vivo* absorption. However, further increasing of FA graft ratio to 19.84% led to no further improvement in insulin absorption, and no significant difference in PA was found between the Ins/PBCA/FA_{19.84}-CS/HA NPs and Ins/PBCA/FA_{12.51}-CS/HA NPs ($p > 0.05$), indicating FA-mediated transport was saturated at the graft ratio 12.51% studied here. And this phenomenon is in good agreement with the *in ex-vivo* permeation results.

3.9. Toxicity studies

Moreover, the *in vivo* safety of nano-delivery system was evaluated by histopathology examination. As revealed in Fig. 10, similar with that

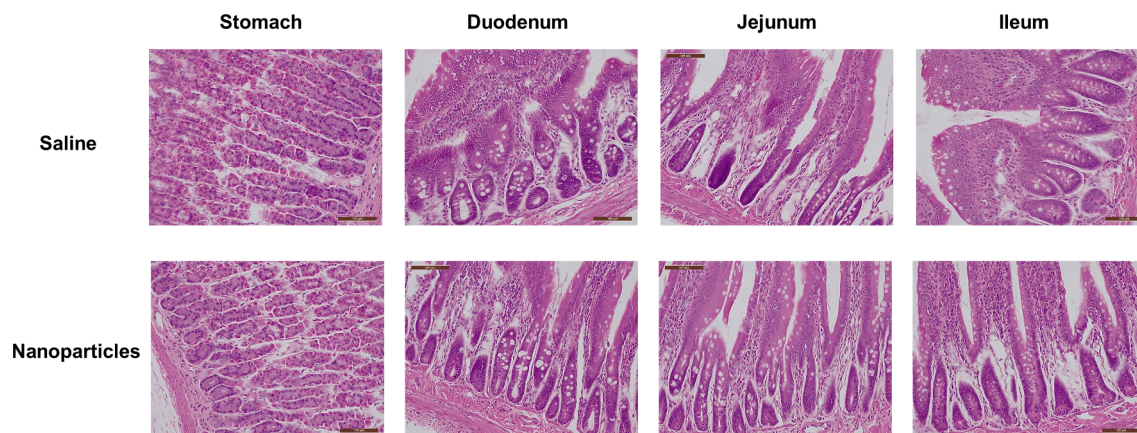


Fig. 10. Gastrointestinal irritation evaluation after the oral administration of Ins/PBCA/FA_{12.51}-CS/HA NPs at dose of 50 IU/Kg for 7 days.

of saline group, no histopathological lesions and hyperemia were observed in the different gastrointestinal segments after 7 days orally administration of Ins/PBCA/FA_{12.51}-CS/HA NPs, indicating the good tissue compatibility and safety of this nano carrier.

4. Conclusion

In order to improve insulin oral delivery efficiency, folic acid decorated virus-mimicking nanoparticles (Ins/PBCA/FACS/HA NPs) were designed herein to overcome both mucus and enterocyte barriers, and the effect of FA-CS graft ratio on insulin intestinal absorption was investigated in rats. It was demonstrated that all the Ins/PBCA/FACS/HA NPs with different FA-CS graft ratio showed good stability and pH-dependent release behavior in the gastrointestinal fluid. And irrespective of the FA-CS graft ratio, the Ins/PBCA/FACS/HA NPs showed similar and excellent penetration in mucus. The nanoparticles permeation in different intestinal segments was FA graft ratio and site dependent, with the best permeation observed in duodenum. Mechanism studies demonstrated that FA carrier-mediated process was involved in the transport of Ins/PBCA/FACS/HA NPs. *In vivo* studies revealed the FA_{12.51}-CS and FA_{19.84}-CS decorated Ins/PBCA/FACS/HA NPs had comparable hypoglycemic effect in diabetic rats. In conclusion, enhanced insulin oral delivery efficiency was indeed achieved by using folic acid decorated virus-mimicking nanoparticles as the carrier, implying mucus penetration in combination with active targeting is an effective way to increase oral insulin absorption, and the ratio of targeting ligand should be optimized.

CRedit authorship contribution statement

Hongbo Cheng: Conceptualization, Methodology, Investigation, Formal analysis, Writing - original draft. **Shuang Guo:** Methodology, Investigation. **Zhixiang Cui:** Validation, Investigation. **Xin Zhang:** Project administration, Software. **Yingnan Huo:** Methodology. **Jian Guan:** Methodology. **Shirui Mao:** Supervision, Conceptualization, Writing - review & editing, Funding acquisition.

Declaration of Competing Interest

The authors declare that they have no known competing financial interests or personal relationships that could have appeared to influence the work reported in this paper.

Acknowledgement

This project is financially supported by the National Natural Science Foundation of China (Grant No. 31870987).

Appendix A. Supplementary material

Supplementary data to this article can be found online at <https://doi.org/10.1016/j.ijpharm.2021.120297>.

References

- Market Research, 2019. Frost&Sullivan Research Reports. <http://www.frostchina.com/wp-content/uploads/2019/09/shengwuyao.pdf>.
- Agrawal, A.K., Urimi, D., Harde, H., Kushwah, V., Jain, S., 2015. Folate appended chitosan nanoparticles augment the stability, bioavailability and efficacy of insulin in diabetic rats following oral administration. *RSC Adv.* 5 (127), 105179–105193.
- Anselmo, A.C., Gokarn, Y., Mitragotri, S., 2019. Non-invasive delivery strategies for biologics. *Nat. Rev. Drug Discov.* 18 (1), 19–40.
- Arbit, E., 2004. The physiological rationale for oral insulin administration. *Diabetes Technol. Ther.* 6 (4), 510–517.
- Cheng, H., Zhang, X., Qin, L., Huo, Y., Cui, Z., Liu, C., Sun, Y., Guan, J., Mao, S., 2020. Design of self-polymerized insulin loaded poly(n-butylcyanoacrylate) nanoparticles for tunable oral delivery. *J. Control. Release* 321, 641–653.
- Dong, W., Wang, X., Liu, C., Zhang, X., Zhang, X., Chen, X., Kou, Y., Mao, S., 2018. Chitosan based polymer-lipid hybrid nanoparticles for oral delivery of enoxaparin. *Int. J. Pharm.* 547 (1–2), 499–505.
- Eilleia, S.Y., Soliman, M.E., Mansour, S., Geneidi, A.S., 2018. Novel technique of insulin loading into porous carriers for oral delivery. *Asian J. Pharm. Sci.* 13 (4), 297–309.
- El Leithy, E.S., Abdel-Bar, H.M., Ali, R.A., 2019. Folate-chitosan nanoparticles triggered insulin cellular uptake and improved *in vivo* hypoglycemic activity. *Int. J. Pharm.* 571, 118708.
- Ensign, L.M., Cone, R., Hanes, J., 2012. Oral drug delivery with polymeric nanoparticles: The gastrointestinal mucus barriers. *Adv. Drug Deliv. Rev.* 64 (6), 557–570.
- Gilli, R., Kacur Kov, M., Mathlouthi, M., Navarini, L., Paoletti, S., 1994. FTIR studies of sodium hyaluronate and its oligomers in the amorphous solid phase and in aqueous solution. *Carbohydr. Res.* 263 (2), 315–326.
- Graf, A., McDowell, A., Rades, T., 2009. Poly(alkylcyanoacrylate) nanoparticles for enhanced delivery of therapeutics - is there real potential? *Expert Opin. Drug Deliv.* 6 (4), 371–387.
- Jin, X., Xu, Y., Shen, J., Ping, Q., Su, Z., You, W., 2011. Chitosan–glutathione conjugate-coated poly(butyl cyanoacrylate) nanoparticles: Promising carriers for oral thymopentin delivery. *Carbohydr. Polym.* 86 (1), 51–57.
- Kaklotar, D., Agrawal, P., Abdulla, A., Singh, R.P., Mehata, A.K., Singh, S., Mishra, B., Pandey, B.L., Trigunayat, A., Muthu, M.S., 2016. Transition from passive to active targeting of oral insulin nanomedicines: enhancement in bioavailability and glycemic control in diabetes. *Nanomedicine* 11 (11), 1465–1486.
- Lai, S.K., Wang, Y.Y., Hanes, J., 2009. Mucus-penetrating nanoparticles for drug and gene delivery to mucosal tissues. *Adv. Drug Deliv. Rev.* 61 (2), 158–171.
- Li, J., Huang, P., Chang, L., Long, X., Dong, A., Liu, J., Chu, L., Hu, F., Liu, J., Deng, L., 2013. Tumor targeting and pH-responsive polyelectrolyte complex nanoparticles based on hyaluronic acid-paclitaxel conjugates and Chitosan for oral delivery of paclitaxel. *Macromol. Res.* 21 (12), 1331–1337.
- Li, L., Liu, Y., Wang, J., Chen, L., Zhang, W., Yan, X., 2016. Preparation, *in vitro* and *in vivo* evaluation of bexarotene nanocrystals with surface modification by folate-chitosan conjugates. *Drug Deliv.* 23 (1), 79–87.
- Liu, C., Kou, Y., Zhang, X., Cheng, H., Chen, X., Mao, S., 2017. Strategies and industrial perspectives to improve oral absorption of biological macromolecules. *Expert Opin. Drug Deliv.* 15 (3), 223–233.
- Liu, C., Kou, Y., Zhang, X., Dong, W., Cheng, H., Mao, S., 2019a. Enhanced oral insulin delivery via surface hydrophilic modification of chitosan copolymer based self-assembly polyelectrolyte nanocomplex. *Int. J. Pharm.* 554, 36–47.
- Liu, C., Xu, H., Sun, Y., Zhang, X., Cheng, H., Mao, S., 2019b. Design of Virus-Mimicking Polyelectrolyte Complexes for Enhanced Oral Insulin Delivery. *J. Pharm. Sci.* 108 (10), 3408–3415.

- Liu, M., Zhang, J., Shan, W., Huang, Y., 2015. Developments of mucus penetrating nanoparticles. *Asian J. Pharm. Sci.* 10 (4), 275–282.
- Malhaire, H., Gimel, J.-C., Roger, E., BENO, T.J.-P., LAGARCE, F., 2016. How to design the surface of peptide-loaded nanoparticles for efficient oral bioavailability? *Adv. Drug Deliv. Rev.* 106, 320–336.
- Olmsted, S.S., Padgett, J.L., Yudin, A.I., Whaley, K.J., Moench, T.R., Cone, R.A., 2001. Diffusion of macromolecules and virus-like particles in human cervical mucus. *Biophys. J.* 81 (4), 1930–1937.
- Pearson, J.P., Chater, P.I., Wilcox, M.D., 2016. The properties of the mucus barrier, a unique gel—how can nanoparticles cross it? *Ther. Deliv.* 7 (4), 229–244.
- Qiu, A., Jansen, M., Sakaris, A., Min, S.H., Chattopadhyay, S., Tsai, E., Sandoval, C., Zhao, R., Akabas, M.H., Goldman, I.D., 2006. Identification of an intestinal folate transporter and the molecular basis for hereditary folate malabsorption. *Cell* 127 (5), 917–928.
- Roger, E., Lagarce, F., Garcion, E., Benoit, J.P., 2010. Biopharmaceutical parameters to consider in order to alter the fate of nanocarriers after oral delivery. *Nanomedicine (Lond)* 5 (2), 287–306.
- Sulheim, E., Baghirov, H., von Haartman, E., Boe, A., Aslund, A.K., Morch, Y., Davies Cde, L., 2016. Cellular uptake and intracellular degradation of poly(alkyl cyanoacrylate) nanoparticles. *J. Nanobiotechnol.* 14, 1.
- Sullivan, C.O., Birkinshaw, C., 2004. In vitro degradation of insulin-loaded poly (n-butylcyanoacrylate) nanoparticles. *Biomaterials* 25 (18), 4375–4382.
- Wang, L., Sun, Y., Shi, C., Li, L., Guan, J., Zhang, X., Ni, R., Duan, X., Li, Y., Mao, S., 2014. Uptake, transport and peroral absorption of fatty glyceride grafted chitosan copolymer–enoxaparin nanocomplexes: Influence of glyceride chain length. *Acta Biomater.* 10 (8), 3675–3685.
- Wong, C.Y., Al-Salami, H., Dass, C.R., 2017. Potential of insulin nanoparticle formulations for oral delivery and diabetes treatment. *J. Control. Release* 264, 247–275.
- Xie, S., Gong, Y.C., Xiong, X.Y., Li, Z.L., Luo, Y.Y., Li, Y.P., 2018. Targeted folate-conjugated pluronic P85/poly(lactide-co-glycolide) polymersome for the oral delivery of insulin. *Nanomedicine (Lond)* 13 (19), 2527–2544.
- Xu, B., Jiang, G.H., Yu, W.J., Liu, D.P., Liu, Y.K., Kong, X.D., Yao, J.M., 2017. Preparation of poly(lactic-co-glycolic acid) and chitosan composite nanocarriers via electrostatic self assembly for oral delivery of insulin. *Mater. Sci. Eng. C Mater. Biol. Appl.* 78, 420–428.
- Yang, C., Gao, S., Kjemis, J., 2014. Folic acid conjugated chitosan for targeted delivery of siRNA to activated macrophages in vitro and in vivo. *J. Mater. Chem. B* 2 (48), 8608–8615.
- Zhang, X., Cheng, H., Dong, W., Zhang, M., Liu, Q., Wang, X., Guan, J., Wu, H., Mao, S., 2018. Design and intestinal mucus penetration mechanism of core-shell nanocomplex. *J. Control. Release* 272, 29–38.
- Zhang, Z., Huey Lee, S., Feng, S. S., 2007. Folate-decorated poly(lactide-co-glycolide)-vitamin E TPGS nanoparticles for targeted drug delivery. *Biomaterials* 28(10), 1889–1899.